Focus on the importance of the process parameters: Temperature cycles and “shock” water addition during the phase inversion process for the formulation of lipid nanoparticles

Claire Gazaille, Sonia Pîgleşan, Kristóf Apró, Laura Ruesche, Aouatef Foudi, Adélie Mellinger, Benjamin Siegler, Joël Eyer, Laurent Lemaire, Patrick Saulnier, et al.

Focus on the importance of the process parameters: Temperature cycles and "shock" water addition during the phase inversion process for the formulation of lipid nanoparticles

Claire Gazaille,[1] Sonia Pîgleşan,[1] Kristóf Apró,[1] Laura Ruesche,[1] Aouatef Foudi,[1] Adélie Mellinger,[1] Benjamin Siegler,[2] Joël Eyer,[1] Laurent Lemaire,[1,3] Patrick Saulnier,[1] Florence Franconi,[1,3] Guillaume Bastiat[1,*]

1 – Univ Angers, INSERM, CNRS, MINT, SFR ICAT, F-49000 Angers, France.

2 – Univ Angers, ASTRAL, SFR MATRIX, F-49000 Angers, France.

3 – Univ Angers, PRISM, SFR ICAT, Biogenouest, F-49000 Angers, France.

* – Corresponding author: guillaume.bastiat@univ-angers.fr

Keywords

Lipid nanoparticles, phase inversion temperature method, size distribution, encapsulation stability, cell viability.

Abstract

The phase inversion temperature method is one of the formulation processes to elaborate nanomedicine based on lipid nanoparticles. This process was used in numerous studies in literature, changing the nature of the ingredients to ensure good encapsulation efficiencies of various drugs. While the product quality attributes to develop various nanomedicines were largely explored, the process parameters remained unchanged from the first lipid nanoparticles designed with this process 25 years ago. It is always composed of 3 temperature cycles and a fast addition of cold water, creating an "irreversible shock" to obtain the lipid nanoparticle in suspensions. To date, the exact roles of these 2 steps remain unclear. We decided to explore their impact by changing the number of temperature cycles and by modifying the final addition of water (temperature, salinity, with or without). Using these various conditions, the size distribution and stability, the capacity of encapsulation and the cytotoxic property of the lipid nanoparticles were compared. It demonstrated the indispensableness of these parameters: at least 1 temperature cycle and rapid cooling and dilution of the mixture, to obtain the most performant nano-systems.

1. Introduction

Lipid nanoparticles (LNP), one of the nanovectors used for many years in attempts to develop nanomedicine, have seen renewed interest with the COVID-19 pandemic and the successful clinical development of mRNA vaccines [1]. Numerous manufacturing processes are reported in the literature, both batch processes such as the self-nanoemulsifying drug delivery systems [2], and continuous processes using microfluidic systems [3].

One of the batch formulation processes used to develop LNP is based on the phase-inversion temperature (PIT) method first described in the late sixties by Shinoda *et al.* [4]. Heurtault *et al.* adapted this concept to develop LNP based on an oily core surrounded by a mixed layer of lecithins and a pegylated surfactant, and patented the process [5-7]. Basically, under magnetic stirring, three cycles of progressive heating and cooling are performed, between 65 and 95°C, on the mixture of three main components: oil (initially Labrafac® WL1349), non-ionic surfactants (initially Lipoid® S75-3 and Kolliphor® HS-15), and salted water. High conductivity values were obtained at low temperature corresponding to an aqueous continuous phase: an oil-in-water (o/w) emulsion while at high temperature, low conductivity values (close to 0 mS/cm) were obtained meaning that the continuous phase is the oil, so a water-in-oil (w/o) emulsion. This phase inversion was defined in a temperature range, a phase inversion zone (PIZ), corresponding to a micro-emulsion state, where no dispersed and continuous phase can be observed [5]. During the last cooling, in the PIZ (about 75°C using the initial components), a rapid addition of cold (4°C) pure water is operated. In the patent and the first publications regarding the LNP formulation process, the role the water addition is confused. The authors defined the operation as a dilution process that breaks off the microemulsion state, leading to an irreversible shock and the LNP formation [5-7]. Depending on the proportion of oil and non-ionic surfactants, the LNP size can be controlled (hydrodynamic diameter range from 25 to 100 nm), with a very narrow size distribution. These LNP characteristics are very well controlled with this solvent-free, soft-energy method, and a good stability profile in an aqueous environment for up to 18 months was maintained [5-7].

Over the past two decades, the LNP were extensively used as nanomedicines for various pre-clinical applications: cancer (liver, lung, brain), inner ear therapies, drug oral administration, etc. The surfactant monolayer structure and the oily core of LNP allowed amphiphilic and lipophilic drugs, respectively, to be easily incorporated inside the nanocarriers. So a large

variety of drugs have been loaded in LNP such as amiodarone [8], ibuprofen [9], indinavir [10], etoposide [11], paclitaxel [12-16], tripentone [17], Sn38 [18], Rhenium complex [19, 20], derivatives of 4-hydroxy tamoxifen combined with ferrocene [21-24], cannabidiol [25], albendazole [26], amphiphilic-modified 5-FU [27], amphiphilic modified gemcitabine [28-30]. Moreover, iron oxide [31], fluorinated molecules [32], or electron paramagnetic resonance probes [33], were encapsulated in LNP to visualize their distribution or assess oxygenation after *in vivo* administration. Finally, biological systems were loaded or adsorbed in the core or at the surface, respectively, of LNP such as targeting peptides [34,35], antimicrobial peptides [36,37], DNA [38,39], and siRNA [40-43].

For this purpose, the formulation was modified in terms of components to perform these drug-loaded LNP depending on the drug properties such as the solubility in the oil core and the capacity to be adsorbed at the LNP surface. For example, Labrafac® WL1349 was replaced by Captex® 8000 to ensure a better paclitaxel or albendazole encapsulation rate [12-16, 26], or by Ethyl Oleate® leading to higher loading of iron oxide [31]. Using the classical components, Cholesterol, Span® 80, glycerol monolaurate or a mixture of 1,2-dioleoyl-sn-glycero-3-phosphoethanolamine (DOPE) / 1,2-dioleoyl-3-trimethylammoniumpropane (DOTAP) was added to improve the encapsulation rate of idinavir [10], amphiphilic modified gemcitabine and 5-FU [27-30], antimicrobial peptides [36,37], or nucleic acid materials [24, 38, 39, 42]. Complexes of DNA were encapsulated in LNP using an additional surfactant: oleic plurol® with Kolliphor® HS-15 and permitted an incorporation of DNA complex inside LNP at moderate temperature, without affecting the biological effect [38,39]. In addition, Béduneau *et al.* replaced Kolliphor® HS-15 with DUB SPEG 30S®: a surfactant with a longer PEG chain, to improve their furtivity in the systemic circulation [44]. To load Sn38, Roger *et al.* totally modified the formulation components with the use of Transcutol® HP as surfactant and Labrafil® M 1944 CS as oil since the drug is not soluble in Labrafac® WL1349 [18].

The only common features of this non-exhaustive list of drug-loaded LNP are the formulation steps when using the phase inversion process. Whatever the component modifications, the protocol always consisted of temperature cycles (usually 3 cycles, although some studies have modified this number [45]) around the microemulsion state, followed by the irreversible shock by the rapid dilution with an aqueous phase (containing additives or not) at the ZIP temperature usually.

In this study, the role and the importance of the number of temperature cycles as well as the rapid cold dilution with pure water were shown and a simplified PIT method was defined. Using the standard compounds: Labrafac® WL1349, Lipoid® S75-3 and Kolliphor® HS-15, four LNP sizes with hydrodynamic diameters of 25, 50, 75 and 100 nm were studied. The various batches of LNP performed with classic and simplified formulation protocols were compared in terms of size distribution, stability, capacity for the encapsulation of model molecules, cytotoxic behavior and the presence of nano-impurities (such as surfactant micelles). All these experiments led to new advances in the comprehension about the phase inversion temperature method and the importance of the irreversible shock.

2. Material and Methods

2.1. LNP formulation

The amounts of Labrafac® WL 1349 (Lab) (triglycerides of caprylic and capric acids) (Gattefossé S.A., Saint-Priest, France) (oil phase); water (Milli-Q plus® system, Millipore, Billerica, MA, USA) and NaCl (Sigma–Aldrich, Saint-Quentin-Fallavier, France) (aqueous phase); and Kolliphor® HS 15 (Kol) (mixture of free polyethylene glycol 660 and polyethylene glycol 660 hydroxystearate) (BASF, Ludwigshafen, Germany) and Lipoïd® S75-3 (Lip) (soybean lecithin: mainly phosphatidylcholine (69%) and phosphatidylethanolamine (10%)) (Lipoïd GmbH, Ludwigshafen, Germany) (surfactants) were precisely weighted ($\pm$ 2 mg).

i) For 25-nm diameter LNP (LNP25): m_{Lab} = 0.568 g, m_{Kol} = 1.299 g, m_{Lip} = 0.050 g, m_{Water} = 3.022 g and m_{NaCl} = 0.089 g;
ii) for 50-nm diameter LNP (LNP50): m_{Lab} = 1.028 g, m_{Kol} = 0.846 g, m_{Lip} = 0.075 g, m_{Water} = 2.962 g and m_{NaCl} = 0.089 g;
iii) for 75-nm diameter LNP (LNP75): m_{Lab} = 1.150 g, m_{Kol} = 0.730 g, m_{Lip} = 0.075 g, m_{Water} = 2.956 g and m_{NaCl} = 0.089 g; and
iv) for 100-nm diameter LNP (LNP100): m_{Lab} = 1.209 g, m_{Kol} = 0.484 g, m_{Lip} = 0.075 g, m_{Water} = 3.143 g and m_{NaCl} = 0.089 g.

For the standard formulation process, the mixtures were heated to 90°C (about 3°C/min) under stirring followed by cooling at the same rate to 50°C. For the standard process, three

successive cycles were performed and during the last cooling, when the temperature of the mixture was in the PIZ (about 75°C), 10 mL of cold (4°C) water was added under stirring.

Other formulation processes were also performed for the LNP50-based mixture. One or 2 successive temperature cycles were performed under stirring, followed by the addition of 10-mL, cold water in the PIZ during the last cooling. Also, 3 successive temperature cycles were performed under stirring, followed by the addition of 10-mL, cold (4°C) water during the last cooling when the temperature of the mixture was at 90, 50 or 20°C. Finally, 3 successive temperature cycles were performed under stirring followed by the addition of 10-mL, hot (90°C) or cold and salted (4°C and NaCl 30 mg/mL) or hot and salted (90°C and NaCl 30 mg/mL) water, in the PIZ during the last cooling.

Finally, a simplified formulation process was performed using LNP25, LNP50, LNP75 and LNP100-based mixtures. It consisted of only one temperature cycle from room temperature to 90°C, at about 3°C/min under stirring, followed to the return to room temperature, without addition of the final water in the PIZ. Ten mL of water were added at the end of the simplified process to have the same LNP concentration as the other LNP suspensions obtained with the standard and the modified processes.

The LNP suspensions (LNPX Std. and LNPX Smp. for the standard and the simplified processes, respectively, with X = 25, 50, 75 and 100; and all the LNP50 obtained with the modified processes) were only purified using filtration through a 0.45-µm Merck Millex™ filter (Thermo Fisher Scientific) and stored at 4°C before use.

2.2. Conductivity measurements

The conductivity of the mixtures was studied during the last temperature cooling, under stirring, using a conductimeter Consort C561 (Consort nv, Turnhout, Belgium) equipped with a conductivity cell K10/Pt1000 (Thermo Fisher Scientific) for the standard process, and the process with the addition of hot and salted (90°C and NaCl 30 mg/mL) water, for the LNP50-based formulation. Moreover, after these 2 processes, the conductivity of the LNP50 suspensions was measured again increasing the temperature.

2.3. Study of LNP batches mixtures

LNP25, LNP50 and LNP100 suspensions obtained with the standard process were mixed with a ratio LNP25/LNP50 of 10/1 (*v/v*) and LNP25/LNP100 of 20/1 (*v/v*). NaCl was added in each mixture to reach a concentration of 30 mg/mL, and one temperature cycle was performed until 90°C, at about 3°C/min under stirring, followed to the return to room temperature. Moreover, 2 mixtures were prepared, precisely weighting all the ingredients.

i) For Mix1, m_{Lab} = 0.609 g, m_{Kol} = 1.256 g, m_{Lip} = 0.052 g, m_{Water} = 12.994 g and m_{NaCl} = 0.045 g.

ii) For Mix2, m_{Lab} = 0.598 g, m_{Kol} = 1.258 g, m_{Lip} = 0.051 g, m_{Water} = 13.005 g and m_{NaCl} = 0.45 g.

Mix1 and Mix2 corresponded to all the ingredients of the mixtures LNP25/LNP50 10/1 (*v/v*) and LNP25/LNP100 20/1 (*v/v*), respectively, before formulation. One temperature cycle (from room temperature to 90°C, at about 3°C/min under stirring, followed to the return to room temperature), without addition of the final water in the PIZ, was done for Mix1 and Mix2.

2.4. Size distribution measurements

The hydrodynamic diameter (Z-ave and intensity size distribution), the polydispersity index (PdI) and the derived count rate (DCR) for the LNP batches or LNP mixtures (see part 2.3.) were determined at 25°C using a Zetasizer® Nano ZS (Malvern Panalytical Ltd., Worcestershire, UK). The instrument is equipped with a 4 mW Helium–Neon laser, with an output wavelength of 633 nm, and a scatter angle fixed at 173°. The LNP suspensions after the various formation processes were diluted by a factor of 60 (*v/v*) with pure water, and the correlation functions were fitted using an exponential fit (Cumulant approach) for Z-ave and PdI determinations. Moreover, the DCR measurements were performed to confirm the presence of LNP in suspensions before and after centrifugation (see part 2.5.). Regarding the mixtures of LNP suspensions, LNP25/LNP50 and LNP25/LNP100 were diluted by a factor 10 and 6 (*v/v*) with pure water, respectively, before the measurements, and the correlation functions for the LNP batches mixtures were fitted using the CONTIN model to evaluate the intensity size distributions.

2.5. Encapsulation stability assay of model molecules

Fluorescent dyes were used as model molecules. To obtain fluorescent-labeled LNP, the various dyes were dissolved in Lab, at concentration of 1 mg/g for both Nile Red (NR) (Sigma–Aldrich) and 1,1'-dioctadecyl-3,3,3',3'-tetramethylindocarbocyanine perchlorate (DiI) (Thermo Fisher Scientific, Illkirch-Graffenstaden, France), prior to perform the standard or simplified formulation process for the LNP25, LNP50 and LNP75-based mixtures. The LNP suspensions were mixed with Lab as a lipophilic external compartment (EC), with the ratio Lab in EC / Lab in LNP of 2 and 5 (*w/w*). The mixtures were vortexed during 15 sec at room temperature, then centrifuged (1,500 g, 30 min). Once complete separation was obtained, the DCR values of the aqueous LNP suspension phase were measured (see part 2.4.). Moreover, the fluorescence intensities were measured on both LNP suspensions and EC phases, using a microplate reader CLARIOstar Plus (BMG Labtech SARL, Champigny-sur-Marne, France), with adequate excitation and emission wavelength couples (λex–λem), *i.e.* 515-590 and 544-590 nm for NR and DiI, respectively. Titration curves with dye-loaded LNP and dye solubilized in EC (determination coefficient higher than 0.99) were performed before evaluating the concentration of dyes in each phase after the encapsulation stability assay.

2.6. F98 and GL261 glioblastoma cell line cultures and viability assays

The F98 and GL261 glioblastoma cell lines (ATCC, Manasas, VA, USA) were grown in Dulbecco's Modified Eagle's medium (DMEM) high glucose (Sigma-Aldrich) supplemented with 10 % fetal bovine serum (Biowest, Nuaillé, France), 1 % antibiotics (10 units of penicillin, 10 mg of streptomycin, Biowest). Cell lines were cultured according to ATCC protocol and maintained at 37°C in a humidified atmosphere with 5% CO_2.

Glioblastoma cells were seeded onto 96-well plates at a density of 5 x 10^4 cells/well and pre-cultured overnight. The cells were treated with LNP suspensions (LNP25, LNP50 or LNP75 obtained with standard or simplified processes) at concentrations ranging from 0.03 to 30 mg/mL for 24 h. After removing the LNP, the viability assays were performed using resazurin (Sigma-Aldrich). Briefly, 100 µL of medium and 20 µL of the resazurin solution (0.15 mg/mL in water) were added in each well and the plates were incubated à 37°C for 3.5 h, in a humidified

atmosphere with 5% CO_2. Then the fluorescence intensities of the wells were measured using a microplate reader CLARIOstar Plus, with an adequate excitation and emission wavelength couple (λex–λem), *i.e.* 560-590 nm. The cell viability percentage was calculated as followed:

$$\text{Cell viability (\%)} = \frac{\text{I}_{\text{LNP-treated cells}} - \text{I}_{\text{without cell}}}{\text{I}_{\text{non-treated cells}} - \text{I}_{\text{without cell}}} \times 100$$

with $I_{LNP\text{-treated cells}}$ the fluorescence intensity of the LNP-treated cells, $I_{non\text{-treated cells}}$ the fluorescence intensity of the non-treated cells and $I_{without\ cells}$ the fluorescence of empty wells.

2.7. Diffusometry by Nuclear Magnetic Resonance (NMR) spectroscopy

Deuterated water (D_2O) (Sigma–Aldrich) was added in non-loaded or NR-loaded or DiI-loaded LNP50 Std. and LNP50 Smp. suspensions with a ratio 1/9 (*v/v*) for frequency locking purpose. ^{1}H NMR pulsed field gradient acquisition, also called diffusion-ordered spectroscopy (DOSY), was performed at 25°C with a 500 MHz AVANCE III HD spectrometer (Bruker, Wissembourg, France) equipped with a 5 mm-Broadband Observe probe at the ASTRAL NMR core facility from Angers University. Diffusion experiments were performed using the stimulated echo sequence with longitudinal Eddy current delay (LED), *ledgp2s*. A series of spectra was acquired with increasing diffusion weighting created by two diffusion magnetic field gradient pulses with increasing intensities, inducing a signal attenuation that depends upon the diffusion coefficients D of the different species that contribute to the signal). When several diffusing species are present, this decay is described by an multiexponential equation of the form: $S(b) = \int f(D) \cdot \exp(-D \cdot b) \cdot dD$ where b is called the diffusion-weighted factor and f(D) the distribution function. b is expressed as: $b = \gamma^2 \cdot g^2 \cdot \delta^2 \cdot (\Delta - \delta/3)$, with γ the gyromagnetic ratio, g the gradient intensity, δ the gradient duration and Δ the separation between the two gradient lobes corresponding to the diffusion observation time. The acquisition parameters were chosen as already described to optimally evaluate diffusion coefficients of all the species present in the mixture while minimizing the relaxation times impact on contribution quantification [46]. The diffusion time Δ was 400 ms, the diffusion gradient duration δ was 20 ms (b_{max}=1178309s/mm²), the gradient shape ramp was linear with 128 steps and the number of averages was 8. The gradient magnitude ranged from 2 to 95% of the maximum gradient intensity (50 G/cm). The whole dataset signal was analyzed using the multivariate SCORE

algorithm from the DOSYToolbox to decompose it into a set of component spectra with associated apparent diffusion coefficients and contributions of each component to the total signal [47, 48].

2.9. Statistical analysis

The statistical analysis of the data was performed using non-parametric tests Mann-Whitney (2 groups) or Kruskal-Wallis followed by Dunn's *post-hoc* test for pairwise comparisons when necessary (more than 2 groups). Significant differences were considered for p-value lower than 0.05.

3. Results and discussion

3.1. Size distribution of LNP in suspension obtained with standard process *vs* modified and simplified ones

To design LNP in suspension, the formulation protocol based on a PIT method is particularly appealing because considered as a free organic solvent, soft-energy method [5, 6]. Referring to Heuthault's patent [7], the standard process consisted of 3 temperature cycles from 50 to 90°C operated on the initial mixture of all the components (surfactants: Kol and Lip, oil: Lab and aqueous phases: NaCl and Water) (**Figure 1A**). These temperature cycles allow to pass from an oil-in-water emulsion at low temperature to a water-in-oil emulsion at high temperature, with an intermediate PIZ, as illustrated with the conductivity profile with high conductivity values (about 20mS/cm) and conductivity values close to 0 mS/cm at low and high temperatures, respectively (**Figure 1B**), as already described [5]. This phase inversion is possible thanks to Kol, a hydrophilic PEGylated non-ionic surfactant, whose HLB value decreases when both temperature and salinity are increased [49], with the cloud point in aqueous solution also observed for other PEGylated surfactants [50]. The cycles are followed by a rapid addition of cold deionized water during the last cooling at the PIZ temperature (about 75°C). After this step considered as a "shock and irreversible" action as described in the patent [7], the suspensions quickly reach a conductivity value close to 5 mS/cm, with the disappearance of the phase inversion phenomenon since the conductivity profile no longer

changes with increasing temperature. This “shock and irreversible” action is also a dilution step and the NaCl concentration is too low (about 7 mg/mL) to allow the phase inversion (PIZ occurs at temperature higher than 100°C) [5]. This process was then considered irreversible and led to LNP suspensions with controlled hydrodynamic diameter with a very narrow size distribution (usually PdI values lower than 0.1). LNP50 suspensions can be obtained after the standard formation process with Z-Ave and PdI values of 54 $\pm$ 1 nm and 0.05 $\pm$ 0.02 (**Figure 1C**). Nevertheless, various formulation parameters can be controlled during this process: the number of temperature cycles, the temperature of the suspension when the “shock” step was operated, and the nature of the water added during this “shock and irreversible” step.

The role of the number of temperature cycles was scarcely studied in the literature. The standard formation process was modified by reducing the number of temperature cycles to 2 and 1, and maintaining constant the other formulation parameters (**Figure 1A**). Considering conductivity profiles as representative of the formulation pathway, the latter is not fundamentally altered by the number of cycles. As expected, alternating high and low conductivities are observed during the temperature cycles, separated by the PIZ transition. Upon the “shock” step, whatever the number of cycles, a rapid change of conductivity profile curves was observed between 75°C and room temperature, with a PIZ shifted towards higher temperatures (**Figure 1B**). After the cycles-modified formulation processes, LNP suspensions were also obtained with Z-Ave and PdI values of 55 $\pm$ 3 nm and 0.06 $\pm$ 0.02 for 2 temperature cycles and 55 $\pm$ 2 nm and 0.06 $\pm$ 0.02 for 1 temperature cycle, respectively, without significant difference compared to the LNP suspension characteristics obtained with the standard process (**Figure 1C**).

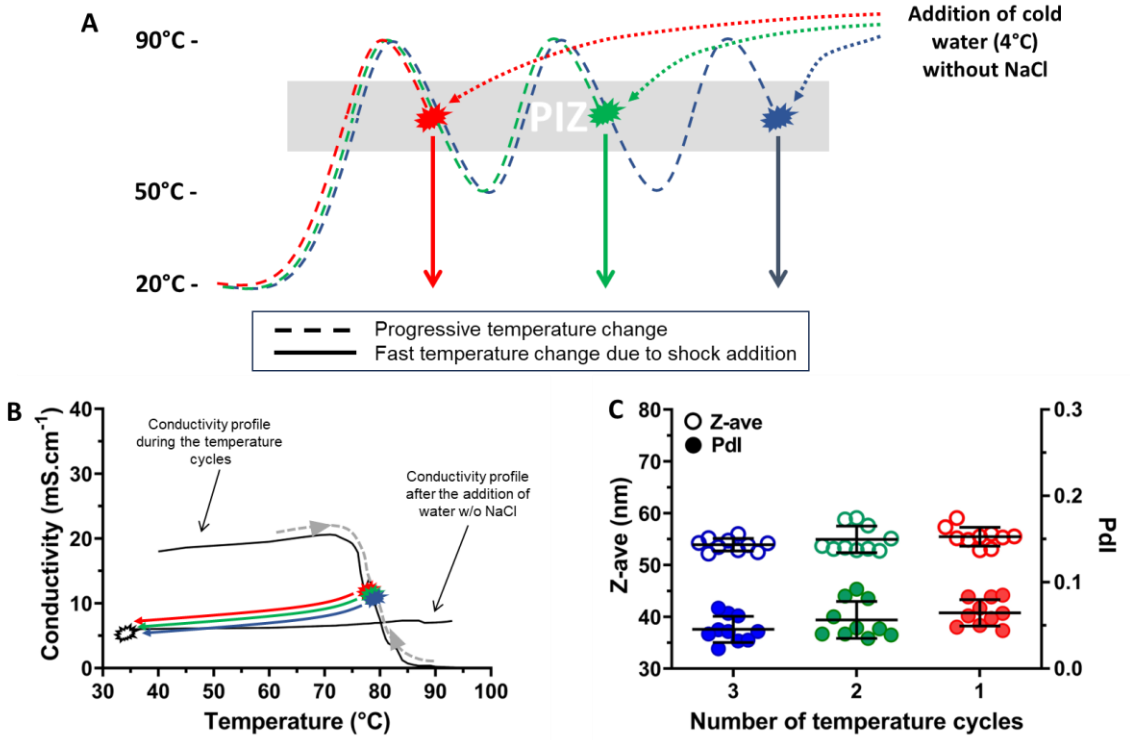

Figure 1. Effect of the number of temperature cycles during the formulation process on the LNP suspension characteristics. A) Diagram of the LNP suspension formulation process and formulation pathways according to the number of temperature cycles considered: blue, green and red lines for 3, 2 and 1 temperature cycles, respectively (PIZ: phase inversion zone). B) Representative conductivity profiles *versus* temperature during the temperature cycles and after the addition of cold deionized water, with the formulation pathways: blue, green and red arrows, corresponding to the number of temperature cycles. C) Size distributions: Z-ave and PdI values of LNP in suspension, obtained with the standard formulation process (3 temperature cycles) and the modified ones (1 and 2 temperature cycles) (n = 10; mean ± SD).

In addition, the role of the temperature of the mixture when cold deionized water is added was studied, and the standard formation process was modified focusing on 3 temperatures: 90, 50 or 20°C, without modifying the other formulation steps (**Figure 2A**). The formulation pathway is not fundamentally modified when water is added at 90°C. There is a rapid change of conductivity profile curves from 90°C to room temperature and a rapid crossing of the PIZ since it is moved towards higher temperatures (**Figure 2B**). When cold water was added at 90°C, a temperature outside and higher than the standard PIZ one (about 75°C), LNP suspensions were obtained with a size distribution comparable to LNP obtained with the standard process: Z-Ave and PdI values of 54 ± 1 nm and 0.06 ± 0.02, respectively (**Figure 2C**). For the other temperatures: 50 and 20°C, the formulation pathway is now totally different:

the rapid change of conductivity profile curves is done after the PIZ is slowly crossed during the last temperature cycle (**Figure 2B**). When cold water was added outside the PIZ but at temperature lower than the standard PIZ one, LNP suspensions were also obtained with a slight but significant increase in size distribution (both for Z-Ave and PdI values). Z-Ave and PdI values were 68 ± 4 nm ($p < 0.0001$) and 0.10 ± 0.01 ($p < 0.0001$) ("shock and irreversible" step at 50°C), and 64 ± 3 nm ($p = 0.0025$) and 0.08 ± 0.02 ($p = 0.0017$) ("shock and irreversible" step at 20°C), respectively (**Figure 2C**). So, the change in the formulation pathway appears to impact the size distribution of the LNP in suspension.

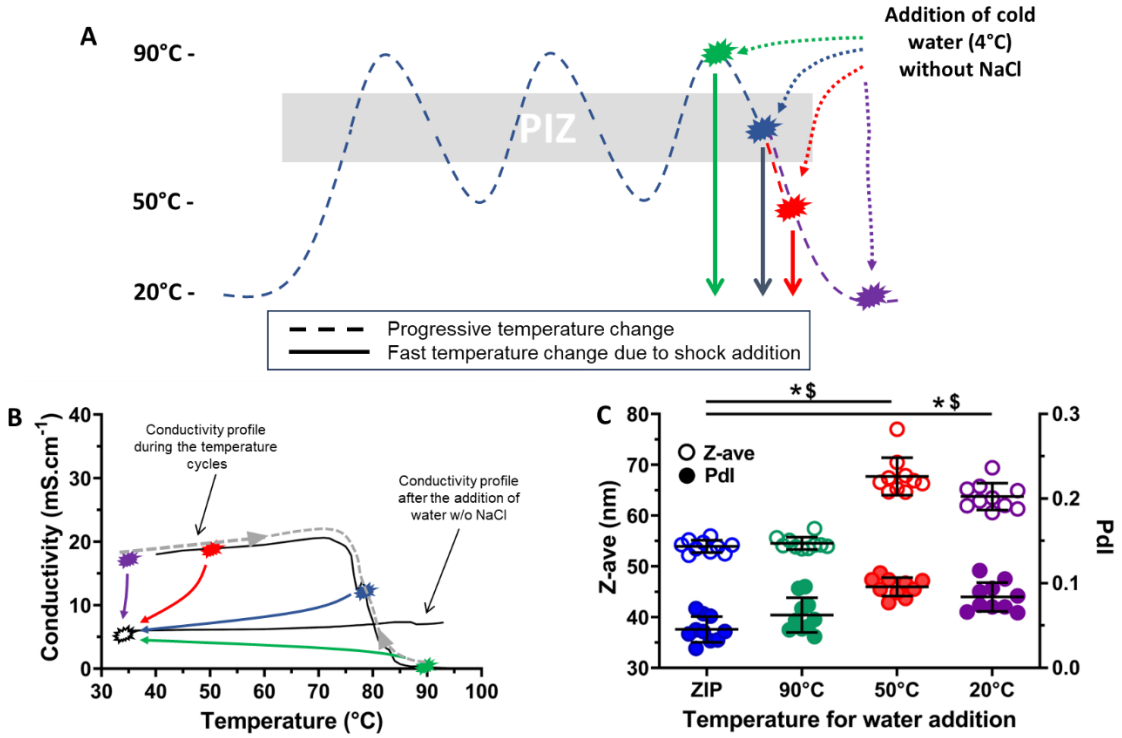

Figure 2. Effect of the temperature of the mixture when the "shock and irreversible" step was operated during the formulation process on the LNP suspension characteristics. A) Diagram of the LNP suspension formulation process and formulation pathways according to the considered temperature of the suspension when the "shock" step was operated: green, blue, red and purple lines for 90, 75, 50 and 20°C, respectively (PIZ: phase inversion zone). B) Representative conductivity profiles *versus* temperature during the temperature cycles and after the addition of cold deionized water, with the formulation pathways: green, blue, red and purple arrows, corresponding to the temperature of the mixture when the "shock" step was operated. C) Size distributions: Z-ave and PdI values of LNP in suspension, obtained with the standard formulation process in blue (cold deionized water added at 75°C) and the modified ones (cold deionized water added at 90, 50 and 20°C in green, red and purple respectively) (n = 10; mean ± SD; Z-ave comparison: ✶ $p < 0.05$; PdI comparison: $ $p < 0.05$).

Finally, the role of the nature of the water added during the “shock and irreversible” step, also never studied in literature to our knowledge, was checked. The standard formation process was modified using deionized water at 90°C, salted water (NaCl 30 mg/mL) at 4°C or 90°C, maintaining unchanged the other formulation parameters (**Figure 3C**). The formulation pathway does not seem fundamentally altered when deionized water at 90°C is added during the PIZ. There is a rapid crossing of the PIZ since it is moved towards higher temperatures and so a rapid change of conductivity profile curves before to progressively return to room temperature (**Figure 3B**). After this modified process, LNP suspensions were also obtained but with a slight and significant increase in size distribution. Z-Ave and PdI values were 66 $\pm$ 4 nm ($p < 0.0001$) and 0.07 $\pm$ 0.01 ($p = 0.0184$) (**Figure 3C**). When NaCl 30 mg/mL solution is added during the PIZ (corresponding to the NaCl concentration of the initial mixture), there is a new conductivity profile with a slight shift of PIZ to higher temperature due to higher NaCl concentration in the final suspension (**Figure 3B**). The formulation pathway appears to be different depending on the temperature of the salted solution. When cold NaCl 30 mg/mL solution is added during the PIZ, there is a rapid change of conductivity towards room temperature, accompanied with a slight move of PIZ to higher temperature. When hot NaCl 30 mg/mL solution is added during the PIZ, as the conductivity profile curves is changed, a slow crossing this new PIZ is observed during the progressive return to room temperature (**Figure 3B**). The results in LNP size distribution are totally different depending on these 2 last modified processes. When cold NaCl 30 mg/mL was added, LNP suspensions were obtained with Z-Ave and PdI values of 55 $\pm$ 2 nm and 0.05 $\pm$ 0.01, without significant difference comparing to the LNP suspension characteristics obtained with the standard process. But when hot NaCl 30 mg/mL was added, the size distribution of LNP in suspension was slightly but significantly increased: Z-Ave and PdI values of 60 $\pm$ 1 nm ($p = 0.0025$) and 0.07 $\pm$ 0.01 ($p = 0.0017$), respectively (**Figure 3C**).

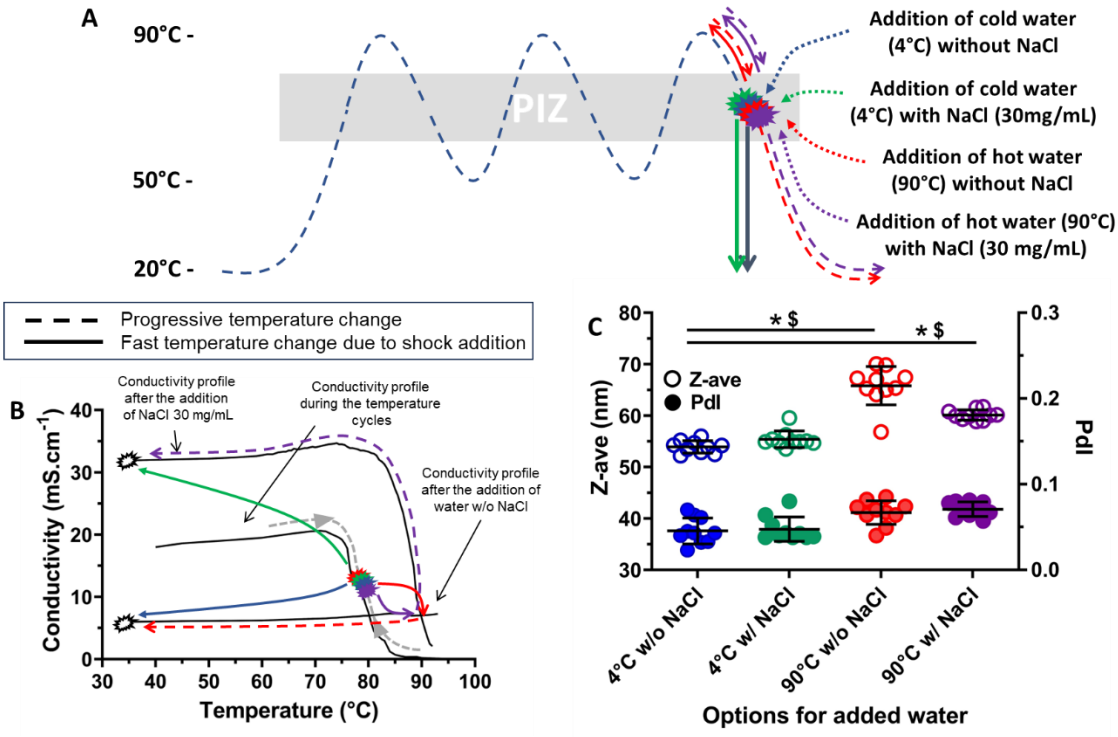

Figure 3. Effect of the nature of the water added during the "shock and irreversible" step during the formulation process on the LNP suspension characteristics. A) Diagram of the LNP suspension formulation process and formulation pathways according to the nature of the water added during the "shock" step: blue, green, red and purple lines for deionized water at 4°C, NaCl 30 mg/mL at 4°C, deionized water at 90°C, and NaCl 30 mg/mL at 90°C, respectively (PIZ: phase inversion zone). B) Representative conductivity profiles *versus* temperature during the temperature cycles, after the addition of cold or hot deionized water, and after the addition of cold or hot NaCl 30 mg/mL, with the formulation pathways: blue, green, and purple arrows, corresponding to the nature of the water added during the "shock" step. C) Size distribution: Z-ave and PdI values of LNP in suspension, obtained with the standard formulation process (deionized water: w/o NaCl at 4°C) and the modified ones (deionized water: w/o NaCl at 90°C, and NaCl 30 mg/mL: w/ NaCl at 4°C or 90°C) (n = 10; mean ± SD; Z-ave comparison: ✶ $p < 0.05$; PdI comparison: $ $p < 0.05$).

Some comments and discussions on the formulation process to design LNP in suspension can already be validated before going any further. First, the number of temperature cycles has no effect on size distribution, and only 1 temperature cycle is needed (**Figure 1C**). Anton *et al.* explored the outer part of the feasibility diagram originally defined for these LNP ingredients by Heurtault *et al.* [6], investigating other oil-, water- and surfactant-phase compositions [45]. They showed that the number of temperature cycles had a direct impact on the final size distribution of the LNP when the compositions were outside the initial feasibility diagram. Nevertheless, within the feasibility diagram, they also showed that only one single

temperature cycle seems sufficient and would only serve to blend ingredients perfectly. It could also explain why a simple microfluidic device, used at room temperature, based on a oil-in-water mixture process can be used to design these LNP [51]. Nevertheless, batch processes are not totally abandoned [52]. In addition, regarding the results for the modified processes, it appears that the combination of both i) a fast return to room temperature, using cold aqueous phase for the "shock and irreversible" step, and ii) a fast crossing of PIZ whatever the NaCl concentration: 0 or 30mg/mL, leads to LNP suspensions with similar size distribution to that of obtained with the standard process (**Figure 1C**: green, blue and red distributions; **Figure 2C**: green distribution, and **Figure 3C**: green distribution). The fast return to room temperature alone (**Figure 2C**: red and purple distribution) or the fast crossing of PIZ alone (**Figure 3C**: red distribution) leads to slight but significant increase in Z-ave and PdI values.

Because the differences in size distribution were not so large considering all the modified protocol we studied: less than 15nm in terms of hydrodynamic diameter, with PdI doubled but still below 0.1, we decided to simplify the formulation protocol as much as possible. We compared the standard protocol: 3 temperature cycles between 50 and 90°C, followed by the "shock and irreversible" step with the rapid addition of cold deionized water during the PIZ, with the simplified one: 1 temperature cycle between of 50 and 90°C, and no "shock and irreversible" step (**Figure 4A**). To respect the concentration, once at room temperature, the LNP suspensions made with the simplified protocol were diluted with the same volume added for the "shock and irreversible" step of the standard protocol. Three other LNP size distributions were targeted: 25, 75 and 100 mn (LNP25, LNP75 and LNP100, respectively), in addition to the previous one: 50 nm (LNP50). Whatever the process used, no major difference was observed for the smallest size distributions. For LNP25 and LNP75, no significant difference was observed between Z-ave values: 27 $\pm$ 1 *versus* 27 $\pm$ 1 nm and 77 $\pm$ 3 *versus* 78 $\pm$ 3 nm for standard *versus* simplified process, respectively. For LNP50, a significant but slight increase in Z-ave was observed: 54 $\pm$ 1 *versus* 61 $\pm$ 2 nm ($p < 0.0001$) for standard *versus* simplified process, respectively. For these various size distributions, the PdI values were lower than 0.1. A large difference between the 2 processes can be observed regarding the LNP100. While the standard process led to the expected LNP size distribution: Z-Ave value of 101 $\pm$ 5 nm and PdI value of 0.06 $\pm$ 0.01, a large and significant increase in size distribution was obtained with the simplified process: Z-Ave value of 138 $\pm$ 11 nm ($p < 0.0001$) and PdI value

of 0.16 ± 0.07 ($p < 0.0001$) (**Figure 4B**). With this last composition, we are at the limit of the feasibility diagram described by Heurtault *et al*. [6]. Design of LNP with monomodal and monodisperse size distributions, using lower surfactant compositions or higher oil proportions, is impossible using the standard protocol. The number of temperature cycles must be increased to improve the size distribution [45], explaining the failure of the simplified process for the LNP100-based mixture. But although the size distributions of LNP25, LNP50 and LNP75 appear similar whatever the formulation process, are there any differences in the behavior of these LNP?

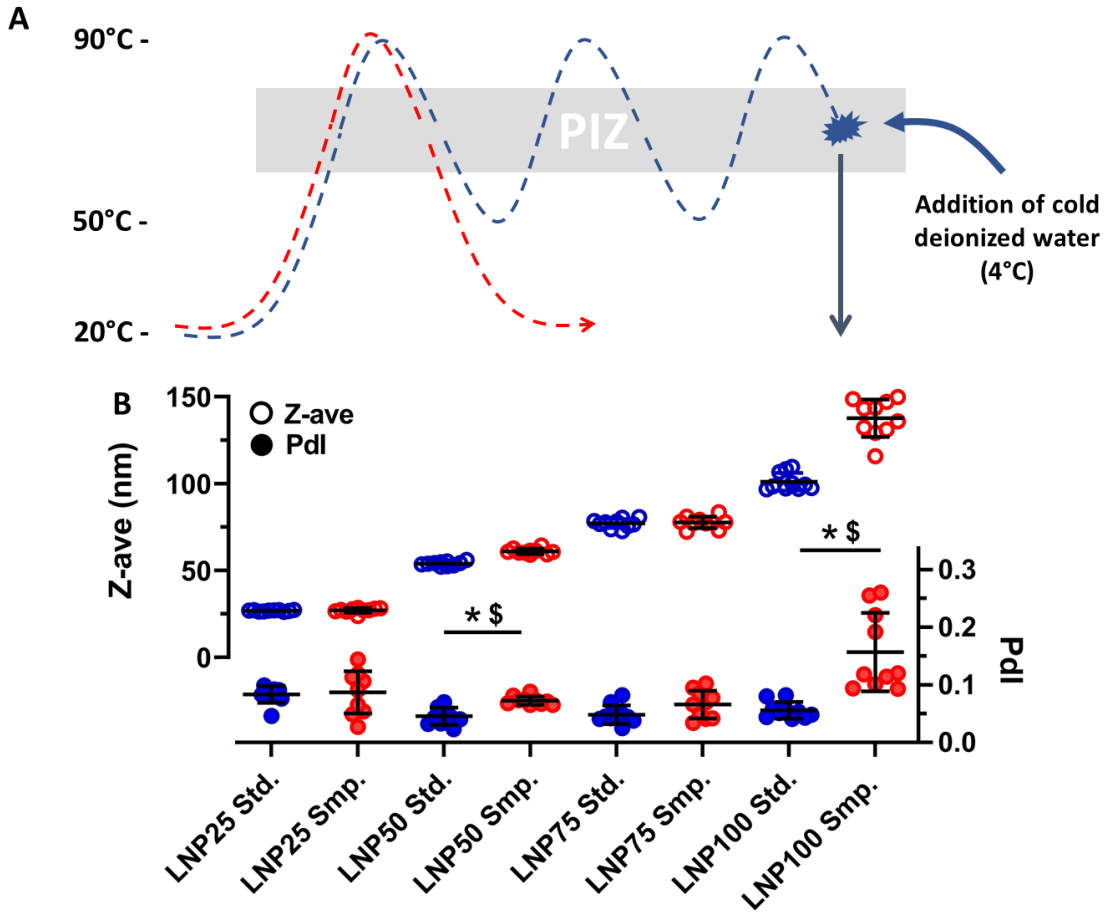

Figure 4. Effect of the simplified formulation process on the LNP suspension characteristics. A) Diagram of the LNP suspension formulation process and formulation pathways for the standard process and the simplified one (PIZ: phase inversion zone). B) Size distributions: Z-ave and PdI values of LNP in suspension, with various expected hydrodynamic diameters: 25, 50, 75 and 100 nm, obtained with the standard formulation process (LNP25 or 50 or 75 or 100 Std.) or the simplified one (LNP25 or 50 or 75 or 100 Smp.) (n = 10; mean ± SD; Z-ave comparison: ✶ $p < 0.05$; PdI comparison: $ $p < 0.05$).

3.2. Cytotoxicity of LNP obtained with standard process *vs* simplified one

The cell viabilities of glioblastoma cells: GL261 and F98 cell lines, were evaluated after 24-h treatment with the LNP in suspension. Whatever the size distribution of the LNP: 25, 50 and 75 nm, and whatever the process for the formulation: the standard or the simplified one, the mean of IC50 values were comprised between 1 and 3 mg/mL for GL261 cell line (**Figure 5A**) and between 0.8 and 2 mg/mL for F98 cell lines (**Figure 5B**). Comparable IC50 values characterized by different assays are commonly found for various cell lines, regardless of LNP size [53]. Even if significant differences for IC50 values were observed: 2.4 ± 0.4 *versus* 1.5 ± 0.6 mg/mL ($p = 0.0011$) for LNP50 Std. *versus* LNP50 Smp., and 2.7 ± 0.4 *versus* 1.9 ± 0.4 mg/mL ($p = 0.0007$) for LNP75 Std. *versus* LNP75 Smp., both for GL261 cell line; 1.3 ± 0.5 *versus* 0.9 ± 0.3 mg/mL ($p = 0.0355$) for LNP25 Std. *versus* LNP25 Smp., for F98 cell line, the slight increases of toxicity regarding the LNP made with the simplified method is really very weak, and could be neglected when cytotoxic drugs will be loaded in LNP.

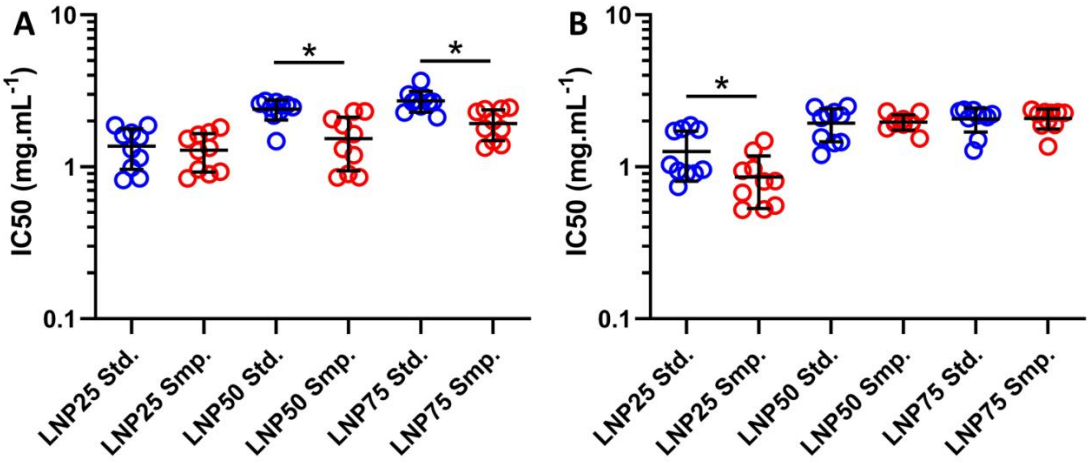

Figure 5. Effect of the formulation process on cell viability. IC50 values (resazurin assay) for LNP in suspension, with various expected hydrodynamic diameters: 25, 50 and 75 nm, obtained with the standard formulation process (LNP25 or 50 or 75 Std.) or the simplified one (LNP25 or 50 or 75 Smp.), after 24-h treatment with glioblastoma cells: A) GL261 and B) F98 cell lines (n = 10; mean ± SD; ✶ $p < 0.05$).

3.3. Encapsulation stability assay of model molecules in LNP obtained with standard process *vs* simplified one

Two model molecules usually used to tag the LNP: NR and DiI, were loaded in LNP25, LNP50 and LNP75, implemented with the standard or the simplified process. LNP100 were excluded from the stability assay due to the failure of the simplified process for the LNP100-based mixture. NR and DiI model molecules have intrinsic lipophilic and amphiphilic properties, respectively, that influence their position in the LNP, and therefore their encapsulation stabilities [54]. First of all, for each model molecule, the same encapsulation rate was considered whatever the process because comparable fluorescence intensities were measured (data not shown).

On the other hand, the size distributions of LNP were modified by the formulation processes. A general increase in mean Z-ave values was observed when the simplified method was implemented, with a loss of monodispersity of the size distributions. These effects are also more pronounced when NR was loaded in LNP in comparison to the other model molecule (**Figure 6**). For instance, the loading of NR in LNP25-based mixture led to an increase of few nm of the mean of Z-ave values when using the standard process while there were significant increases of the means of both Z-ave (1.4-fold, $p < 0.0001$) and PdI (2.5-fold, $p < 0.0001$) values, when using the simplified one (**Figure 6A**).

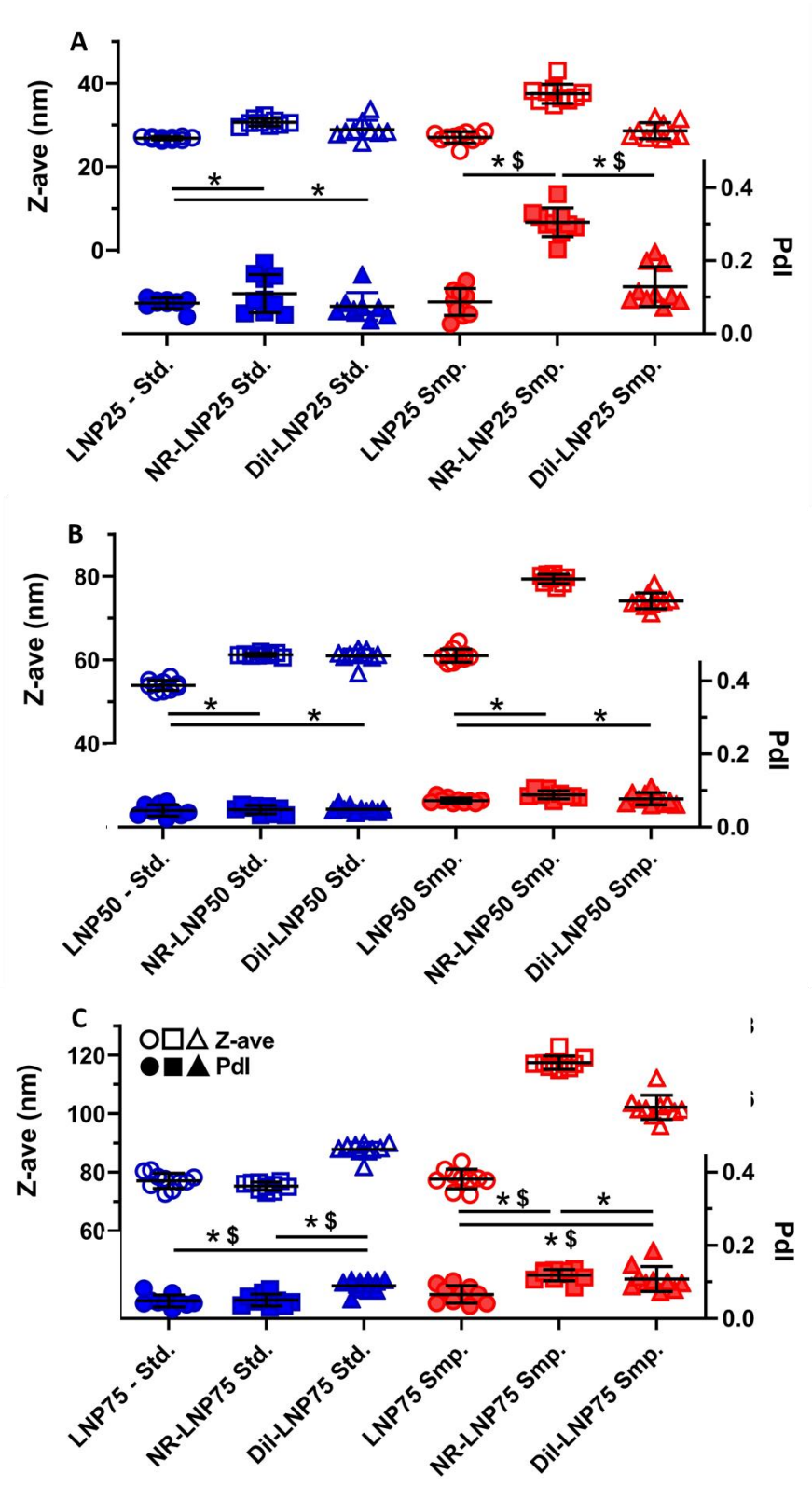

Figure 6. Effect of the formulation process on the model molecule-loaded LNP suspension size distributions. Size distributions: Z-ave and PdI values of non-loaded and NR or DiI-loaded LNP in suspension, with various expected hydrodynamic diameters: 25 (A), 50 (B), and 75 nm (C), obtained with the standard formulation process (LNP25 or 50 or 75 Std.) or the simplified one (LNP25 or 50 or 75 Smp.) (n = 10; mean ± SD; Z-ave comparison: ✶ $p < 0.05$; PdI comparison: \$ $p < 0.05$).

Moreover, the loading of NR or DiI in LNP75-based mixture also led to an increase of few nm of the mean of Z-ave values when using the standard process while there were significant increases of the means of both Z-ave (1.5-fold, $p < 0.0001$; and 1.3-fold, $p = 0.0332$) and PdI (1.8-fold, $p = 0.0003$; and 1.6-fold, $p = 0.0287$) values, when using the simplified one, for NR and DiI loadings, respectively (**Figure 6C**). The same observations were made with the NR and DiI loadings in the LNP50-based mixture (**Figure 6B**).

As Heurtault *et al.* describe with their empirical model, these increases in LNP size could be due to a partial participation of surfactants in the LNP structure [6]. Indeed, some of these surfactants could be mobilized to enable solubilization of lipophilic model molecules within process residual micelles in the aqueous phase, and this consequence would be more pronounced in the simplified process.

The stability of loading was studied using a transfer assay already described for these 2 molecules [54], using an external lipophilic compartment able to create a partition for the lipophilic molecules between itself and LNP. As already described, we observed the NR proportion in LNP decreased, signing an increased release of NR from LNP to the external lipophilic compartment as the volume of the external lipophilic compartment increases whatever the formulation process (**Figure 7A and C**). No difference for NR proportions was observed after the transfer assay for LNP25 and LNP50, depending on the formulation process. Only for LNP75, the proportion of NR still loaded in LNP after the transfer assay was significantly higher when the standard process was used in comparison to the simplified one: 87 ± 4 % *vs* 66 ± 2 % ($p < 0.0001$), respectively, using the lowest volume for the external lipophilic compartment (**Figure 7A**) and 52 ± 3 % *vs* 37 ± 2 % ($p < 0.0001$), respectively, using the highest volume for the external lipophilic compartment (**Figure 7C**). Regarding DiI, it remained totally loaded in the LNP thanks to its amphiphilic property, whatever the formulation process and whatever the volume of the external lipophilic compartment involved during the transfer assay (**Figure 7B and D**), as already reported [52].

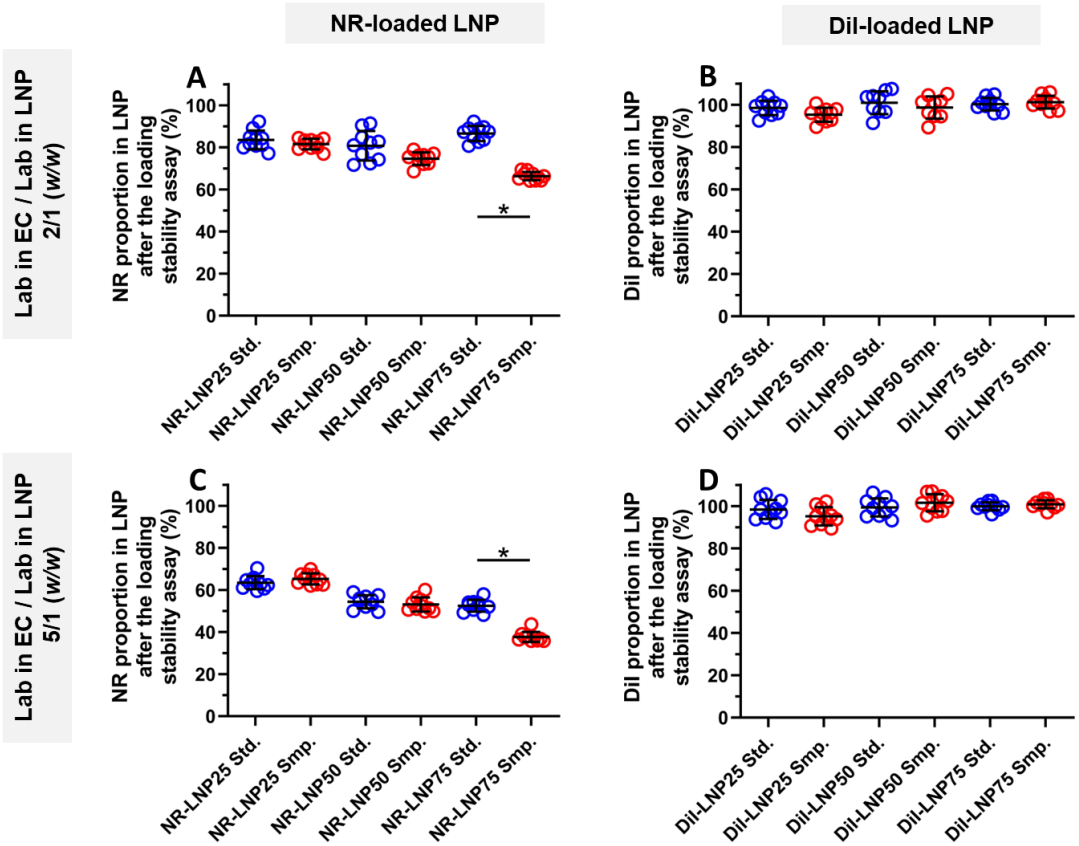

Figure 7. Effect of the formulation process on the loading stability of the model molecules loaded in LNP. Proportions of NR (A/C) and DiI (B/D) still loaded in LNP with various expected hydrodynamic diameters: 25, 50, and 75 nm, obtained with the standard formulation process (LNP25 or 50 or 75 Std.) or the simplified one (LNP25 or 50 or 75 Smp.), after the loading stability assay, using Lab as external lipophilic compartment (EC) with the ratio Lab in EC / Lab in LNP of 2 (A/B) and 5 (*w/w*) (C/D) (n = 10; mean ± SD; ✶ $p < 0.05$).

3.4. Residual micelles in LNP suspensions obtained with standard process *vs* simplified one

^{1}H NMR diffusometry, was done to check the presence of residual micelles after the formulation processes, with LNP50 Std. and LNP50 Smp., but also with the NR and DiI-loaded ones. As already reported for a different LNP [55], three different diffusing species were also observed in all the LNP suspensions: i) a fast diffusing one at about 2.4×10^{-4} mm^2/s, corresponding to free PEG in the suspension and coming from free PEG in commercial Kol; ii) a mild diffusing one at about 0.15×10^{-4} mm^2/s, corresponding to PEG hydroxystearate (Kol) residual micelles in the suspension; and iii) a low diffusing one at about 0.04×10^{-4} mm^2/s, corresponding to LNP.

No difference can be observed for the proportion of apparent ^{1}H NMR signal corresponding to the free PEG (fast diffusion species) as calculated using multivariate SCORE algorithm, whatever the formulation. It corresponds to the free PEG proportion in each formulation, soluble in the aqueous phase, consistent with the same proportion of Kol in each LNP formulation. For the other apparent ^{1}H NMR signal distributions (mild and slow diffusion species), significant differences can be observed (**Figure 8**). For the non-loaded LNP50, the simplified process led to a significantly higher apparent ^{1}H NMR signal proportion of 15.5 $\pm$ 0.9 % *vs* 11.6 $\pm$ 1.1 % ($p < 0.0324$) of residual micelles in the suspension compared to the standard process. This increase is correlated with the decrease of apparent ^{1}H NMR signal proportion in the LNP: 58.4 $\pm$ 1.6 % in the simplified process *vs* 62.4 $\pm$ 1.9 % in the standard process. This effect was also observed with the dye-loaded LNP50 and was more pronounced for NR than DiI. Indeed, for the NR-LNP50, the simplified process led to a significant higher proportion: 19.8 $\pm$ 1.5 % *vs* 13.3 $\pm$ 1.3 % ($p < 0.0022$) of residual micelles in the suspension, correlated with a significant decrease proportion in the LNP: 53.3 $\pm$ 2.1 % *vs* 61.1 $\pm$ 2.1 % ($p < 0.0144$); and for the DiI-LNP50, the simplified process led to a significant higher proportion: 16.8 $\pm$ 0.8 % *vs* 12.4 $\pm$ 1.9 % ($p < 0.0092$) of residual micelles in the suspension, correlated with a decrease of proportion in the LNP: 57.3 $\pm$ 1.1 % *vs* 62.2 $\pm$ 3.1 % ($p < 0.0144$); in comparison to the standard one (**Figure 8**). The lower proportion of Kol in the dye-loaded LNP done with simplified process already suggested regarding their size distribution (**Figure 6**) appears to be confirmed with the diffusometry experiments, even if size modifications induced relaxometry impact on species signal proportion cannot completely be excluded.

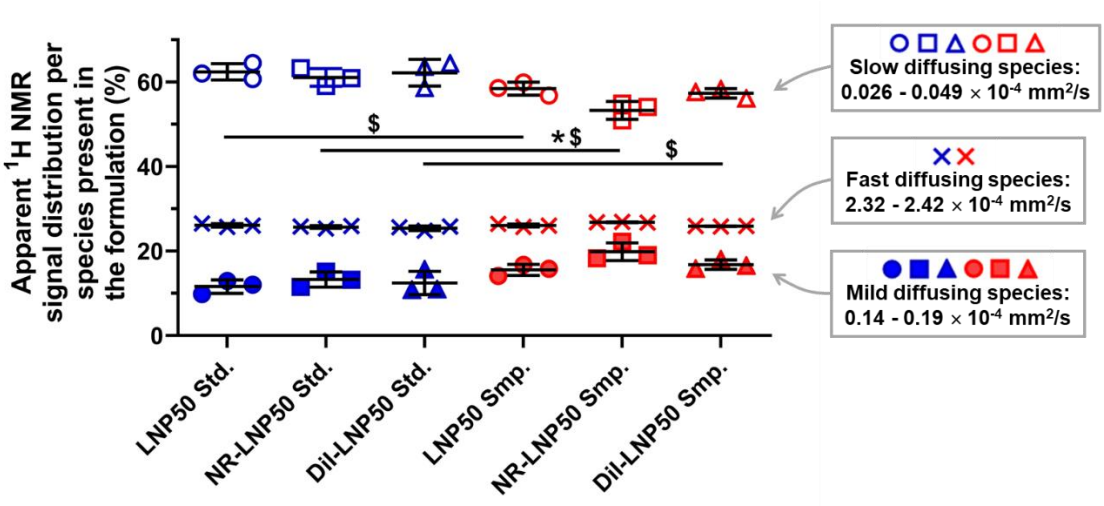

Figure 8. Effect of the formulation process on the presence of residual micelles in LNP suspension. Apparent ^{1}H NMR signal distribution with diffusion coefficient values for diffusing species in non-loaded LNP, NR and DiI-loaded LNP, with expected hydrodynamic diameters of 50 nm, obtained with the standard formulation process (LNP50 or NR-LNP50 or DiI-LNP50 Std.) or the simplified one (LNP50 or NR-LNP50 or DiI-LNP50 Smp.) (n = 3; mean ± SD; slow diffusing species comparison: ✶ $p < 0.05$; mild diffusing species comparison: $ $p < 0.05$).

3.5. Size distribution stability for LNP obtained with standard process *vs* simplified one

Considering the stability of the size distributions of the LNP suspensions (stored at 4°C), another difference between the 2 processes was observed. A slight but not significant increase in size for LNP25, LNP50 and LNP75 was observed with the standard process up to 6 months. On the other hand, a significant increase in Z-ave was observed at 6 months with the simplified process: about 110 nm ($p < 0.0001$) for the LNP75, about 10 nm ($p < 0.0001$) for the LNP50, but not for the LNP25 (**Table 1**). Using the simplified process, LNP instability over time seems to depend on the size of the nano-objects: the larger the LNP, the faster they will destabilize. This could explain why such size differences are observed for LNP100 using the standard process and the simplified process at the end of the formulation process (**Table 1** and **Figure 4**).

Table 1. Effect of the formulation process on the size distribution stability for LNP suspension. Size distribution: Z-Ave and PdI evolution of LNP25, LNP50 and LNP75 obtained after standard (Std.) and simplified (Smp.) processes, stored at 4°C until 6 months (n = 10; mean ± SD; ✶ $p < 0.05$; PdI comparison: $ $p < 0.05$).

			0 month	1 month	2 months	6 months
LNP25	Std. process	Z-Ave (nm)	27 ± 1	28 ± 1	28 ± 1	31 ± 1
		PdI	0.08 ± 0.01	0.07 ± 0.01	0.06 ± 0.02	0.17 ± 0.05
	Smp. process	Z-Ave (nm)	27 ± 1	28 ± 1	26 ± 1	32 ± 1
		PdI	0.09 ± 0.04	0.06 ± 0.02	0.06 ± 0.03	0.17 ± 0.04
LNP50	Std. process	Z-Ave (nm)	54 ± 1	57 ± 1	57 ± 1	59 ± 1
		PdI	0.04 ± 0.02	0.04 ± 0.01	0.04 ± 0.01	0.06 ± 0.02
	Smp. process	Z-Ave (nm)	61 ± 2	65 ± 2	67 ± 2	71 ± 2 ✶
		PdI	0.07 ± 0.01	0.04 ± 0.02	0.06 ± 0.01	0.06 ± 0.01
LNP75	Std. process	Z-Ave (nm)	77 ± 3	75 ± 3	75 ± 3	81 ± 3
		PdI	0.05 ± 0.02	0.06 ± 0.02	0.06 ± 0.02	0.04 ± 0.01
	Smp. process	Z-Ave (nm)	78 ± 3	79 ± 5	80 ± 6	194 ± 126 ✶
		PdI	0.07 ± 0.02	0.08 ± 0.01	0.09 ± 0.01	0.38 ± 0.26 $
LNP100	Std. process	Z-Ave (nm)	101 ± 5			
		PdI	0.06 ± 0.01			
	Smp. process	Z-Ave (nm)	138 ± 11 ✶			
		PdI	0.16 ± 0.07 $			

3.6. Irreversibility for the phase inversion process

The patent and the first publications describing the design of LNP using the phase inversion process also report the concept of irreversibility [5-7]. The final step consisting of the addition of water was considered to lead to an irreversible shock to form the LNP in suspension. Indeed, when the LNP were formulated using the standard process, *i.e.* 4 °C deionized water added into the PIZ, the conductivity dropped and the profile remained constant whatever the temperature of the sample (**Figure 1B**), so there is no possible change in LNP size with temperature variation after the cold dilution. Indeed, as reported previously, the phase inversion temperature depends on NaCl concentration and at this dilution, the PIZ moves to temperature higher than 100 °C [5]. This concept of irreversibility is true in this case, confirming the LNP stability over temperature and no possibility to reach once again a phase inversion with temperature. On the other hand, the nature of the aqueous phase added during the PIZ is important for this concept. When the LNP are formulated with the addition of water containing NaCl 30 mg/mL into the PIZ, the NaCl concentration doesn't change in comparison

to the initial mixture and PIZ is always present (**Figure 3B**). Therefore, modification possibilities of the LNP with temperature variation should persist.

To test this hypothesis, LNP25 and LNP50, obtained with the standard protocol, were mixed at a ratio 10/1 (*v/v*). The resulting size distribution profile presented a monomodal large distribution, combining both individual ones, the sizes of the LNP being too close to be isolated by dynamic light scattering technique. (**Figure 9A**). The same experiment was done mixing LNP25 and LNP100, obtained with the standard protocol, at a ratio 20/1 (*v/v*). The resulting size distribution profile also combined both individual ones, but more visible in this case thanks to the bimodal size distribution (**Figure 9C**). NaCl was added in each mixture at a final concentration of 30 mg/mL and one temperature cycle was performed. The resulting size distribution of the LNP obtained after the temperature cycle was totally different from the initial mixture (**Figure 9B and 9D**). For the mixture LNP25 and LNP100, a monomodal distribution was observed (**Figure 9D**). For the LNP25 and LNP50 mixture, the already monomodal distribution became narrower (**Figure 9B**). After the NaCl addition and the temperature cycle for the LNP mixtures, the 2 LNP crossed a phase transition to be in a water-in-oil emulsion at high temperature, leading to the fusion of the 2 oil phases. Crossing back the phase transition during the temperature decrease, the mixtures of LNP were not maintained resulting to a unique LNP with monomodal size distribution. To control the assumption, all the chemicals used to prepare the mixtures LNP25/LNP50 at a ratio 10/1 (*v/v*) or LNP25/LNP100 at a ratio 20/1 (*v/v*) were individually weighted, and one temperature cycle was applied. The size distributions were the same as the one measured after heating the mixtures (**Figures 9B and 9D**) confirming the fusion between the LNP, and so the limit of the concept of irreversibility when pure water is not used.

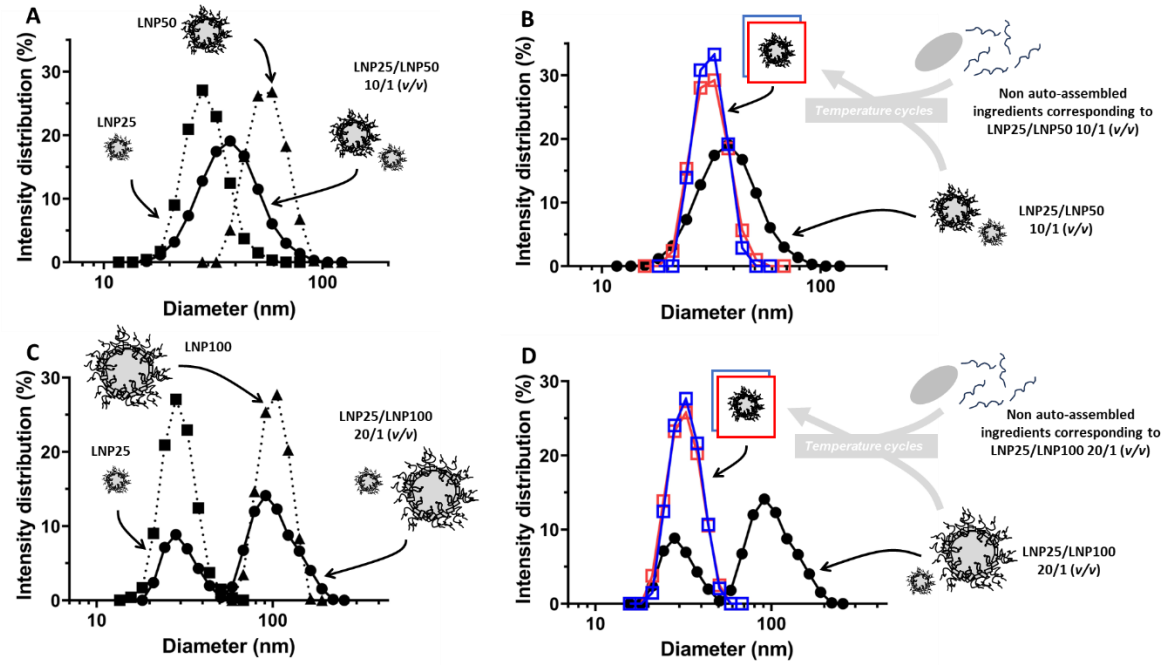

Figure 9. The limit of the concept of irreversibility for the phase inversion process. Size distribution in intensity for A) LNP25 and LNP50 in suspension, obtained with the standard protocol, and the mixture LNP25/LNP50 10/1 (*v/v*); for B) the mixture LNP25/LNP50 10/1 (*v/v*) before and after 1 temperature cycle (red size distribution), and all the individually weighted ingredients corresponding to the same mixture after 1 temperature cycle (blue distribution); for C) the LNP25 and LNP100 in suspension, obtained with the standard protocol, and the mixture LNP25/LNP100 20/1 (*v/v*); and for D) the mixture LNP25/LNP100 20/1 (*v/v*) before and after 1 temperature cycle (red distribution), and all the individually weighted ingredients corresponding to the same mixture after 1 temperature cycle (blue distribution).

4. Conclusion

The phase inversion method to elaborate LNP requires 2 essential steps. First, a temperature cycle is needed to allow the solubilization of the hydrophilic surfactant: Kol, in the oil phase and the simultaneous release of the molecules at the oil-water interface during the cooling step. However, we have shown that only one cycle is sufficient, as long as the hydrophilic surfactant is effectively solubilized in the oil phase, and the 3 cycles described in the literature offer no additional advantage. Second, the rapid addition of cold pure water in the PIZ is also needed and its absence can affect the LNP properties. In terms of significance, we can highlight that the absence of this last step: i) alters the stability of the LNP size distribution; ii) increases the LNP size distribution when encapsulating drug mimicking molecules, iii) increases the presence of residual surfactant not participating in the formulation, iv) alters the stability of

the encapsulation of drug mimicking molecules, and v) increases cytotoxicity. We can hypothesize that the absence of the rapid addition of cold water, replaced by a slow cooling step, provokes a progressive release of surfactants from the oil to the oil-water interface and promotes their escape toward the water phase as we observed more free residual surfactant in the LNP suspensions. When cold water was added, the return to room temperature was faster, provoking an instantaneous release of surfactants to the oil-water interface, blocking them and decreasing their escape from the LNP structure. We also proved that the irreversibility described for this last step is due to the drop in salinity which makes the impossibility to reach again the PIZ rather than a thermal shock by the cold-water addition, even though the dilution is essential for the long-term stability of LNP. Of course, the change in process parameters was only studied for the LNP designed with Kol. Other surfactants with similar properties as Kol could also be tested to generalize our hypothesis. In addition, we studied these parameters only *in vitro*. Because the LNP are used as a platform to elaborate nanomedical strategies, an *in vivo* comparison of the future of the LNP done with the standard and the simplified process, such as pharmacokinetic and biodistribution studies, should be also indicative of the real differences between the 2 nano-systems. In the case of an industrial application in batch, reducing the number of temperature cycles could be a significant factor in scale-up, since it could generate significant energy savings, as well as savings in formulation time. Nevertheless, the batch processes are more and more replaced by continuous ones for the elaboration of that kind of nano-objects, such as microfluidic systems. The processes are no longer based on temperature phase inversion, but on composition phase inversion or spontaneous nano-emulsification, simply mixing at a microscopic scale an oil phase with an aqueous phase. These processes do not propose a rapid cold dilution, the importance of which we have shown for a batch process with temperature phase inversion. It could be interesting to explore the similarities and the differences in the physico-chemical properties and the biological evaluations of the nano-objects obtained by the different methods, to optimize the processes in line with the therapeutic objectives envisaged for the nanomedicines to be developed.

5. CRediT authorship contribution statement

Conceptualization, CG and GB; formal analysis, CG, SP, KA, LR, AF, AM and BS; data analysis, CG, SP, KA, LR, AF, AM, BS, FF; methodology, CG, FF, GB; validation, CG, FF, LL, GB; visualization, CG, FF, GB; funding acquisition, GB; project administration, PS, JE and GB; supervision, JE and GB; writing—original draft, GB; writing—review and editing, LL, FF, GB. All authors have read and agreed to the published version of the manuscript.

6. Declaration of interest statement

The authors declare no competing interest.

7. Acknowledgments

This work was carried out within the research program of GLIOGEL (EuroNanoMed3 - 7th call) (grant agreement no. EURONANOMED2017-082). The authors also thank the *Fondation ARC pour la Recherche sur le Cancer* (grant agreement no. PJA 20161204860) and the *Ligue Contre le Cancer (Comité du Maine-et-Loire et Comité Loire-Atlantique)* (grant agreement no. 270/12.2021). Claire Gazaille acknowledges a scholarship from the *Université d'Angers* and *Angers Loire Métropole*.

8. Data availability

Data will be made available on request.

9. References

[1] P.R. Cullis, P.L. Felgner, The 60-year evolution of lipid nanoparticles for nucleic acid delivery, Nat. Rev. Drug Discov. 23(9) (2024) 709-722. https://doi.org/10.1038/s41573-024-00977-6.

[2] A. Chauhan, R. Kamal, R. Mishra, D. Shekho, A. Awasthi, A Comprehensive Guide to the Development, Evaluation, and Future Prospects of Self-nanoemulsifying Drug Delivery Systems for Poorly Water-soluble Drugs, Curr. Pharm. Des. 30(16) (2024) 1211-1216. https://doi.org/10.2174/0113816128296705240327065131.

[3] S. Mehraji, D.L. DeVoe, Microfluidic synthesis of lipid-based nanoparticles for drug delivery: recent advances and opportunities, Lab. Chip 24(5) (2024) 1154-1174. https://doi.org/10.1039/d3lc00821e.

[4] K. Shinoda K, H. Saito, The Stability of O/W Type Emulsions as Functions of Temperature and the HLB of Emulsifiers: The Emulsification by PIT- method, J. Coll. Inter. Sci. 30(2) (1969) 258-263. https://doi.org/10.1016/S0021-9797(69)80012-3.

[5] B. Heurtault, P. Saulnier, B. Pech, J.E. Proust, J.P. Benoit, A novel phase inversion-based process for the preparation of lipid nanocarriers, Pharm. Res. 19(6) (2002) 875-880. https://doi.org/10.1023/a:1016121319668.

[6] B. Heurtault, P. Saulnier, B. Pech, M.C. Venier-Julienne, J.E. Proust, R. Phan-Tan-Luu, J.P. Benoit JP, The influence of lipid nanocapsule composition on their size distribution, Eur. J. Pharm. Sci. 18(1) (2003) 55-61. https://doi.org/10.1016/s0928-0987(02)00241-5.

[7] B. Heurtault, P. Saulnier, B. Pech, J.E. Proust, J. Richard, J.P. Benoit JP, Patent No. WO02688000 (2000).

[8] A. Lamprecht, Y. Bouligand, J.P. Benoit JP, New lipid nanocapsules exhibit sustained release properties for amiodarone, J. Control. Release 84(1-2) (2002) 59-68. https://doi.org/10.1016/s0168-3659(02)00258-4.

[9] A. Lamprecht, J.L. Saumet, J. Roux, J.P. Benoit JP, Lipid nanocarriers as drug delivery system for ibuprofen in pain treatment, Int. J. Pharm. 278(2) (2004) 407-414. https://doi.org/10.1016/j.ijpharm.2004.03.018.

[10] M. Pereira de Oliveira, E. Garcion, N. Venisse, J.P. Benoit, W. Couet, J.C. Olivier, Tissue distribution of indinavir administered as solid lipid nanocapsule formulation in mdr1a (+/+) and mdr1a (-/-) CF-1 mice, Pharm. Res. 22(11) (2005) 1898-1905. https://doi.org/10.1007/s11095-005-7147-6.

[11] A. Lamprecht, J.P. Benoit JP, Etoposide nanocarriers suppress glioma cell growth by intracellular drug delivery and simultaneous P-glycoprotein inhibition, J. Control. Release 112(2) (2006) 208-213. https://doi.org/10.1016/j.jconrel.2006.02.014.

[12] F. Lacoeuille, F. Hindre, F. Moal, J. Roux, C. Passirani, O. Couturier, P. Cales, J.J. Le Jeune, A. Lamprecht, J.P. Benoit, In vivo evaluation of lipid nanocapsules as a promising colloidal carrier for paclitaxel, Int. J. Pharm. 344(1-2) (2007) 143-149. https://doi.org/10.1016/j.ijpharm.2007.06.014.

[13] E. Garcion, A. Lamprecht, B. Heurtault, A. Paillard, A. Aubert-Pouessel, B. Denizot, P. Menei, J.P. Benoit, A new generation of anticancer, drug-loaded, colloidal vectors reverses multidrug resistance in glioma and reduces tumor progression in rats, Mol. Cancer Ther. 5(7) (2006) 1710-1722. https://doi.org/10.1158/1535-7163.MCT-06-0289.

[14] A. Paillard, F. Hindré, C. Vignes-Colombeix, J.P. Benoit JP, E. Garcion E, The importance of endo-lysosomal escape with lipid nanocapsules for drug subcellular bioavailability, Biomaterials 31(29) (2010) 7542-7554. https://doi.org/10.1016/j.biomaterials.2010.06.024.

[15] E. Roger, F. Lagarce, E. Garcion, J.P. Benoit JP, Reciprocal competition between lipid nanocapsules and P-gp for paclitaxel transport across Caco-2 cells, Eur. J. Pharm. Sci. 40(5) (2010) 422-429. https://doi.org/10.1016/j.ejps.2010.04.015.

[16] J. Hureaux, F. Lagarce, F. Gagnadoux, M.C. Rousselet, V. Moal, T. Urban, J.P. Benoit, Toxicological study and efficacy of blank and paclitaxel-loaded lipid nanocapsules after i.v. administration in mice, Pharm. Res. 27(3) (2010) 421-430. https://doi.org/10.1007/s11095-009-0024-y.

[17] A. Malzert-Fréon, S. Vrignaud, P. Saulnier, V. Lisowski, J.P. Benoit, S. Rault S, Formulation of sustained release nanoparticles loaded with a tripentone, a new anticancer agent, Int. J. Pharm. 320(1-2) (2006) 157-164. https://doi.org/10.1016/j.ijpharm.2006.04.007.

[18] E. Roger, F. Lagarce, J.P. Benoit JP, Development and characterization of a novel lipid nanocapsule formulation of Sn38 for oral administration, Eur. J. Pharm. Biopharm. 79(1) (2011) 181-188. https://doi.org/10.1016/j.ejpb.2011.01.021.

[19] C. Vanpouille-Box, F. Lacoeuille, C. Belloche, N. Lepareur, L. Lemaire, J.J. LeJeune, J.P. Benoit, P. Menei, O.F. Couturier, E. Garcion, F. Hindré F, Tumor eradication in rat glioma and bypass of immunosuppressive barriers using internal radiation with (188)Re-lipid nanocapsules, Biomaterials 32(28) (2011) 6781-6790. https://doi.org/10.1016/j.biomaterials.2011.05.067.

[20] A. Cikankowitz, A. Clavreul, C. Tétaud, L. Lemaire, A. Rousseau, N. Lepareur, D. Dabli, F. Bouchet, E. Garcion, P. Menei, O. Couturier, F. Hindré F, Characterization of the distribution, retention, and efficacy of internal radiation of 188Re-lipid nanocapsules in an immunocompromised human glioblastoma model, J. Neurooncol. 131(1) (2017) 49-58. https://doi.org/10.1007/s11060-016-2289-4.

[21] E. Allard, C. Passirani, E. Garcion, P. Pigeon, A. Vessières, G. Jaouen, J.P. Benoit, Lipid nanocapsules loaded with an organometallic tamoxifen derivative as a novel drug-carrier system for experimental malignant gliomas, J. Control. Release 130(2) (2008) 146-153. https://doi.org/10.1016/j.jconrel.2008.05.027.

[22] E. Allard, N.T. Huynh, A. Vessières, P. Pigeon, G. Jaouen, J.P. Benoit, C. Passirani, Dose effect activity of ferrocifen-loaded lipid nanocapsules on a 9L-glioma model, Int. J. Pharm. 379(2) (2009) 317-323. https://doi.org/10.1016/j.ijpharm.2009.05.031.

[23] E. Allard, D. Jarnet, A. Vessières, S. Vinchon-Petit, G. Jaouen, J.P. Benoit, C. Passirani, Local delivery of ferrociphenol lipid nanocapsules followed by external radiotherapy as a synergistic treatment against intracranial 9L glioma xenograft, Pharm. Res. 27(1) (2010) 56-64. https://doi.org/10.1007/s11095-009-0006-0.

[24] P. Resnier, N. Galopin, Y. Sibiril, A. Clavreul, J. Cayon, A. Briganti, P. Legras, A. Vessières, T. Montier, G. Jaouen, J.P. Benoit, C. Passirani, Efficient ferrocifen anticancer drug and Bcl-2 gene therapy using lipid nanocapsules on human melanoma xenograft in mouse, Pharmacol. Res. 126 (2017) 54-65. https://doi.org/10.1016/j.phrs.2017.01.031.

[25] J. Aparicio-Blanco, V. Sebastián, J.P. Benoit, A.I. Torres-Suárez AI, Lipid nanocapsules decorated and loaded with cannabidiol as targeted prolonged release carriers for glioma therapy: In vitro screening of critical parameters, Eur. J. Pharm. Biopharm. 134 (2019) 126-137. https://doi.org/10.1016/j.ejpb.2018.11.020.

[26] G.V. Ullio Gamboa, P.E. Pensel, M.C. Elissondo, S.F. Sanchez Bruni, J.P. Benoit, S.D. Palma, D.A. Allemandi, Albendazole-lipid nanocapsules: Optimization, characterization and chemoprophylactic efficacy in mice infected with Echinococcus granulosus, Exp. Parasitol. 198 (2019) 79-86. https://doi.org/10.1016/j.exppara.2019.02.002.

[27] G. Lollo, K. Matha, M. Bocchiardo, J. Bejaud, I. Marigo, A. Virgone-Carlotta, T. Dehoux, C. Rivière, J.P. Rieu, S. Briançon, T. Perrier, O. Meyer, J.P. Benoit, Drug delivery to tumours using a novel 5-FU derivative encapsulated into lipid nanocapsules, J. Drug Target. 27(5-6) (2019) 634-645. https://doi.org/10.1080/1061186X.2018.1547733.

[28] E. Moysan, Y. González-Fernández, N. Lautram, J. Béjaud, G. Bastiat, J.P. Benoit JP, An innovative hydrogel of gemcitabine-loaded lipid nanocapsules: when the drug is a key player of the nanomedicine structure, Soft Matter. 10(11) (2014) 1767-1777. https://doi.org/10.1039/c3sm52781f.

[29] C. Bastiancich, J. Bianco, K. Vanvarenberg, B. Ucakar, N. Joudiou, B. Gallez, G. Bastiat, F. Lagarce, V. Préat, F. Danhier, Injectable nanomedicine hydrogel for local chemotherapy of glioblastoma after surgical resection, J. Control. Release 264 (2017) 45-54. https://doi.org/10.1016/j.jconrel.2017.08.019.

[30] C. Bastiancich, L. Lemaire, J. Bianco, F. Franconi, F. Danhier, V. Préat, G. Bastiat, F. Lagarce, Evaluation of lauroyl-gemcitabine-loaded hydrogel efficacy in glioblastoma rat models, Nanomedicine (Lond) 13(16) (2018) 1999-2013. https://doi.org/10.2217/nnm-2018-0057.

[31] F. Franconi, C. Chapon, J.J. Le Jeune, P. Richomme, L. Lemaire L, Susceptibility gradient quantization by MRI signal response mapping (SIRMA) to dephaser, Med. Phys. 37(2) (2010) 877-884. https://doi.org/10.1118/1.3298019.

[32] L. Lemaire, G. Bastiat, F. Franconi, N. Lautram, T. Duong Thi Dan, E. Garcion, P. Saulnier, J.P. Benoit, Perfluorocarbon-loaded lipid nanocapsules as oxygen sensors for tumor tissue pO_2 assessment, Eur. J. Pharm. Biopharm. 84(3) (2013) 479-486. https://doi.org/10.1016/j.ejpb.2013.01.003.

[33] J. Nel, C.M. Desmet, B. Driesschaert, P. Saulnier, L. Lemaire, B. Gallez B, Preparation and evaluation of trityl-loaded lipid nanocapsules as oxygen sensors for electron paramagnetic resonance oximetry, Int. J. Pharm. 554 (2019) 87-92. https://doi.org/10.1016/j.ijpharm.2018.11.007.

[34] J. Balzeau, M. Pinier, R. Berges, P. Saulnier, J.P. Benoit, J. Eyer J, The effect of functionalizing lipid nanocapsules with NFL-TBS.40-63 peptide on their uptake by glioblastoma cells, Biomaterials 34(13) (2013) 3381-3389. https://doi.org/10.1016/j.biomaterials.2013.01.068.

[35] R. Karim, E. Lepeltier, L. Esnault, P. Pigeon, L. Lemaire, C. Lépinoux-Chambaud, N. Clere, G. Jaouen, J. Eyer, G. Piel, C. Passirani, Enhanced and preferential internalization of lipid nanocapsules into human glioblastoma cells: effect of a surface-functionalizing NFL peptide, Nanoscale 10(28) (2018) 13485-13501. https://doi.org/10.1039/c8nr02132e.

[36] A. Umerska, V. Cassisa, G. Bastiat, N. Matougui, H. Nehme, F. Manero, M. Eveillard, P. Saulnier, Synergistic interactions between antimicrobial peptides derived from plectasin and lipid nanocapsules containing monolaurin as a cosurfactant against Staphylococcus aureus, Int. J. Nanomedicine 12 (2017) 5687-5699. https://doi.org/10.2147/IJN.S139625.

[37] H. Nehme, P. Saulnier, A.A. Ramadan, V. Cassisa, C. Guillet, M. Eveillard, A. Umerska, Antibacterial activity of antipsychotic agents, their association with lipid nanocapsules and its impact on the properties of the nanocarriers and on antibacterial activity, PLoS One 13(1) (2018) e0189950. https://doi.org/10.1371/journal.pone.0189950.

[38] M. Morille, C. Passirani, S. Dufort, G. Bastiat, B. Pitard, J.L. Coll, J.P. Benoit, Tumor transfection after systemic injection of DNA lipid nanocapsules, Biomaterials 32(9) (2011) 2327-2333. https://doi.org/10.1016/j.biomaterials.2010.11.063.

[39] S. David, T. Montier, N. Carmoy, P. Resnier, A. Clavreul, M. Mével, B. Pitard, J.P. Benoit, C. Passirani, Treatment efficacy of DNA lipid nanocapsules and DNA multimodular systems after systemic administration in a human glioma model, J. Gene Med. 14(12) (2012) 769-775. https://doi.org/10.1002/jgm.2683.

[40] E. Bourseau-Guilmain, J. Béjaud, A. Griveau, N. Lautram, F. Hindré, M. Weyland, J.P. Benoit, E. Garcion, Development and characterization of immuno-nanocarriers targeting the cancer stem cell marker AC133, Int. J. Pharm. 423(1) (2012) 93-101. https://doi.org/10.1016/j.ijpharm.2011.06.001.

[41] M. Weyland, A. Griveau, J. Béjaud, J.P. Benoit, P. Coursaget, E. Garcion, Lipid nanocapsule functionalization by lipopeptides derived from human papillomavirus type-16 capsid for nucleic acid delivery into cancer cells, Int. J. Pharm. 454(2) (2013) 756-764. https://doi.org/10.1016/j.ijpharm.2013.06.013.

[42] P. Resnier, P. LeQuinio, N. Lautram, E. André, C. Gaillard, G. Bastiat, J.P. Benoit, C. Passirani, Efficient in vitro gene therapy with PEG siRNA lipid nanocapsules for passive targeting strategy in melanoma, Biotechnol. J. 9(11) (é014) 1389-1401. https://doi.org/10.1002/biot.201400162.

[43] F. Danhier, K. Messaoudi, L. Lemaire, J.P. Benoit, F. Lagarce, Combined anti-Galectin-1 and anti-EGFR siRNA-loaded chitosan-lipid nanocapsules decrease temozolomide resistance in glioblastoma: in vivo evaluation, Int. J. Pharm. 481(1-2) (2015) 154-161. https://doi.org/10.1016/j.ijpharm.2015.01.051.

[44] A. Béduneau, P. Saulnier, N. Anton, F. Hindré, C. Passirani, H. Rajerison, N. Noiret, J.P. Benoit, Pegylated nanocapsules produced by an organic solvent-free method: Evaluation of their stealth properties, Pharm. Res. 23(9) (2006) 2190-2199. https://doi.org/10.1007/s11095-006-9061-y.

[45] N. Anton, P. Gayet, J.P. Benoit, P. Saulnier, Nano-emulsions and nanocapsules by the PIT method: an investigation on the role of the temperature cycling on the emulsion phase inversion, Int. J. Pharm. 344(1-2) (2007) 44-52. https://doi.org/10.1016/j.ijpharm.2007.04.027.

[46] F. Franconi, L. Lemaire, B. Siegler, J.C. Gimel, P. Saulnier, NMR diffusometry data sampling optimization for mixture analysis, J. Pharm. Biomed. Anal. 148 (2018) 156-162. https://doi.org/doi:10.1016/j.jpba.2017.09.028.

[47] M. Nilsson, G.A. Morris, Speedy component resolution: an improved tool for processing diffusion-ordered spectroscopy data, Anal. Chem. 80(10) (2006) 3777-3782. https://doi.org/doi:10.1021/ac7025833.

[48] M. Nilsson, The DOSY Toolbox: a new tool for processing PFG NMR diffusion data, J. Magn. Reason. 200(2) (2009) 296-302. https://doi.org/10.1016/j.jmr.2009.07.022.

[49] L. Hu, J. Zhang, C. Zhu, H.C. Pan, H. Liu, Effect of the additives on clouding behavior and thermodynamics of coenzyme Q10-Kolliphor HS15 micelle aqueous solutions, Chem. Phys. Lett. 687 (2017) 264-269. https://doi.org/10.1016/j.cplett.2017.09.032.

[50] K.S. Sharma, S. R. Patil, A. K. Rakshit, Study of the cloud point of C12En nonionic surfactants: effect of additives, Colloids Surf. A Physicochem. Eng. Asp. 219(1-3) (2003) 67-74. https://doi.org/10.1016/S0927-7757(03)00012-8.

[51] N. Rolley, M. Bonnin, G. Lefebvre, S. Verron, S. Bargiel, L. Robert, J. Riou, C. Simonsson, T. Bizien, J.C. Gimel, J.P. Benoit, G. Brotons, B. Calvignac, Galenic Lab-on-a-Chip concept for lipid nanocapsules production, Nanoscale 13(27) (2021) 11899-11912. https://doi.org/10.1039/d1nr00879j.

[52] S.K. Yadava, B.P.K. Reddy, M.R. Prausnitz, M.T. Cicerone, Hybrid Lipid Nanocapsules: A Robust Platform for mRNA Delivery, ACS Appl. Mater. Interfaces 16(13) (2024) 15981-15992. https://doi.org/10.1021/acsami.4c00992.

[53] G. Le Roux, H. Moche, A. Nieto, J.P. Benoit, F. Nesslany, F. Lagarce, Cytotoxicity and genotoxicity of lipid nanocapsules, Toxicol. In Vitro 41 (2017) 189-199. https://doi.org/10.1016/j.tiv.2017.03.007.

[54] G. Bastiat, C.O. Pritz, C. Roider, F. Fouchet, E. Lignières, A. Jesacher, R. Glueckert, M. Ritsch-Marte, A. Schrott-Fischer, P. Saulnier, J.P. Benoit, A new tool to ensure the fluorescent dye labeling stability of nanocarriers: a real challenge for fluorescence imaging, J. Control. Release 170(3) (2013) 334-342. https://doi.org/10.1016/j.jconrel.2013.06.014.

[55] E. Roger, F. Franconi, T.A.T. Do, C. Simonsson, B. Siegler, R. Perrot, P. Saulnier, J.C. Gimel, Evidence of residual micellar structures in a lipid nanocapsule dispersion. A multi-technique approach, J. Control. Release 364 (2023) 700-717. https://doi.org/10.1016/j.jconrel.2023.10.054.